

Phonon scattering in lightly neutron-irradiated diamond

Donald T. Morelli and Thomas A. Perry

Physics Department, General Motors Research and Environmental Staff, Warren, Michigan 48090-9055

John W. Farmer

Research Reactor, University of Missouri-Columbia, Columbia, Missouri 65211

(Received 22 July 1992)

We report measurements on the thermal conductivity of diamond irradiated with fast neutrons. Low levels of irradiation ($< 10^{19}$ neutrons cm^{-2}) create vacancies and small regions of disordered carbon, whereas heavy doses ($> 10^{20}$ neutrons cm^{-2}) initiate vitrification. In this sense diamond is similar to the well-studied case of irradiated quartz. Our results in the low-dose regime are consistent with additional phonon scattering in the irradiated material by the extended regions of disordered carbon. The size and concentration of these regions are derived from the thermal-conductivity data correlate with those determined from the infrared spectra as well as with those estimated from a radiation-damage model. A comparison is made between the thermal conductivity of the irradiated material and that of synthetic vapor-deposited diamond films.

I. INTRODUCTION

Due to the extraordinarily high thermal conductivity of type-IIa diamond (exceeding $20 \text{ W cm}^{-1} \text{ K}^{-1}$, five times that of copper at room temperature), chemically vapor-deposited (CVD) diamond films have been proposed for many heat-transfer applications. Early studies¹⁻³ indicated, however, that the thermal conductivity of films was no more than half that of single crystals. In recent years, though, the growth of high-quality CVD diamond has proceeded dramatically, and recent reports^{4,5} place the thermal conductivity of diamond films as high as $17 \text{ W cm}^{-1} \text{ K}^{-1}$. While it has been recognized that the lower value for films in comparison to that of a single crystal is due partly to a crystallite size effect,^{6,2} the role of defects in limiting the thermal conductivity has not yet been fully explored. Morelli, Hartnett, and Robinson⁴ noted that films grown by hot-filament vapor deposition had lower room-temperature thermal conductivities than those grown by a microwave process, and exhibited a strong dip in the thermal conductivity between 15 and 60 K. This was attributed to an additional scattering of heat-carrying phonons by either a resonant or a precipitated defect in the hot-filament samples. Candidate defects were sp^2 -bonded carbon, vacancies, or metallic filament impurities. While it has been suggested that there is a correlation between the room-temperature thermal conductivity and the amount of sp^2 -bonded carbon in a diamond film as determined by the ratio of the intensities of the sp^2 and sp^3 -bonded carbon peaks in the Raman spectrum,^{1,3} no such definite trend has been observed. A difficulty in this regard is that vapor-deposited diamond films possess a rich defect spectrum and, in addition to containing sp^2 -bonded carbon, they also may contain, depending on the growth conditions, vacancies, carbon interstitials, hydrogen, nitrogen, and metallic impurities, all of which are capable of influencing the ability of these materials to conduct heat. In addition, the crystallite size

can differ dramatically from film to film and even across the thickness of a single film.⁷ These factors complicate the analysis of thermal-conductivity data in terms of scattering processes to the extent that it is difficult to determine the influence of each type of defect on the thermal conductivity.

One way around this problem is to introduce some of these defects into a diamond single crystal in a controlled and well-determined way and study their influence on the thermal conductivity. The technique we have chosen is irradiation by fast neutrons. For low fluences ($< 10^{19}$ neutrons cm^{-2}) neutrons produce lattice vacancies and small regions of disordered carbon.^{8,9} As the neutron fluence is augmented, the damage increases to the point that for fluences greater than 10^{20} neutrons cm^{-2} , amorphization of diamond develops.^{10,11} Thus two important types of defects in diamond films, vacancies, and regions of disordered carbon, can be produced artificially in a single crystal by neutron irradiation. Furthermore, each of these defects has a characteristic optical signature: a neutral vacancy in diamond luminesces at 1.673 eV, a vacancy complexed with two nitrogen atoms emits light at 2.463 eV when excited, and disordered carbon displays a peak in the Raman spectrum near 1600 cm^{-1} and a continuum of absorption in the one-phonon region of the infrared-absorption spectrum.

Any discussion of defects in natural diamond necessarily must recognize the subtle but important role played by residual nitrogen impurities in determining the ultimate structure of defects in this material. Extensive optical and electron paramagnetic resonance (EPR) experiments have established that nitrogen can exist in three different configurations in the diamond lattice: (1) as isolated substitutional impurities, which produce an EPR signal and infrared absorption at 1130 cm^{-1} ; (2) *A* aggregates, or nitrogen-atom pairs, which are EPR inactive and exhibit infrared absorption at 1282 and 1197 cm^{-1} ; and (3) *B* aggregates, which are larger aggregates of nitrogen atoms

and show infrared absorption at 1175 and 1282 cm^{-1} . Combination of these nitrogen centers with one or more vacancies is the source of the rich optical spectroscopy of diamond, and can provide a powerful tool for characterizing the defect state of an irradiated diamond.

With regard to thermal conductivity, there have been numerous studies on the influence of neutron irradiation on this property of nonmetallic solids. Examples include sapphire,^{12,13} which does not amorphize under any radiation dose, to silicon,¹⁴ which exhibits only a 15% amorphization at a fluence of 10^{21} neutrons cm^{-2} . Perhaps the most well-studied and fascinating system is quartz, which, like diamond, undergoes vitrification upon neutron irradiation, and thus has been the subject of many studies¹⁵⁻¹⁷ which have probed the tunneling nature of heat transport in the amorphous material. Interestingly, while the influence of neutron irradiation on the optical properties of diamond has been studied in great detail,¹⁸ the effect on the thermal conductivity has not been considered.¹⁹ In view of the wealth of information gleaned from such studies on quartz, this situation is quite surprising. The goal of the present set of experiments was to study the optical and thermal properties of diamond at each radiation step in order to determine the influence of various types of defects on the thermal conductivity.

II. EXPERIMENTAL TECHNIQUE

We obtained a single crystal of type-IIa natural diamond from Dubbledee Harris Company. Its dimensions were $2 \times 10 \times 0.25$ mm^3 with the $\langle 100 \rangle$ plane parallel to the slab plane. The crystal was polished on all sides by the supplier. Type-IIa diamonds are characterized by absorption in the infrared portion of the spectrum in the range 1400–4000 cm^{-1} (2.5–7.2 μm). To verify the quality of our diamond, we obtained an infrared spectrum, shown in Fig. 1. The spectrum is typical of that of type-IIa diamond, showing absorption peaks only in the two- and three-phonon regions, with only very weak absorption in the 1100–1330- cm^{-1} range. Due to the sym-

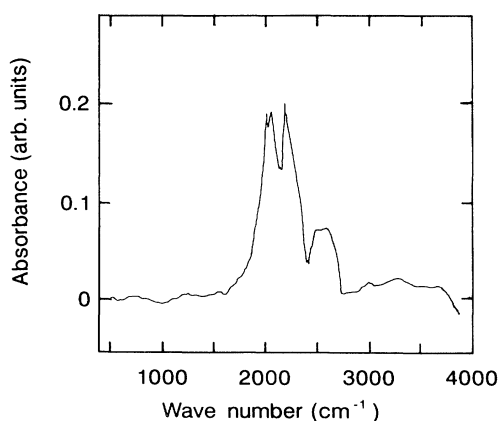


FIG. 1. The infrared-absorption spectrum of natural unirradiated type-IIa single-crystal diamond.

metry of the diamond lattice, one-phonon absorption (< 1330 cm^{-1}) is not allowed.²⁰ However, defects which disrupt the symmetry give rise to single-phonon absorption.^{9,21} The diamond studied here is defect free to the extent that little absorption is observed in this part of the spectrum. The weak absorption in the 1100–1330- cm^{-1} region is due to the presence of nitrogen in the lattice; from the strength of these peaks it is estimated that the total concentration of nitrogen is on the order of 10^{18} cm^{-3} , typical for type-IIa diamond. Detailed examination of the one-phonon region shows that it is of complicated shape, indicating that the nitrogen is present in some mixture of the three possible configurations described above.

Raman and photoluminescence spectra were gathered at room temperature using an ISA double monochromator and an argon-ion laser as the excitation source ($\lambda = 457.9, 467.5, 488.0,$ and 528.7 nm). The source power was 50 mW and was focused using a cylindrical lens; this gave a power density on the order of 10 W cm^{-2} . The quality of the unirradiated diamond can also be judged by its Raman/photoluminescence spectrum (Fig. 2). The Raman spectrum has a single sharp feature at 1331.9 cm^{-1} with a full width at half maximum (FWHM) of 2.22 cm^{-1} ; this is the well-studied zone-center phonon mode of diamond.²² No other Raman features are resolved in this spectrum. In particular, there is no evidence of any scattering near 1360 or 1580 cm^{-1} , regions commonly attributed to sp^2 bonds in the sp^3 lattice. The broad feature beginning just below the laser energy (2.52 eV) and peaking at ~ 2.35 eV (1400- cm^{-1} shift) is a photoluminescence feature. Analysis of this structure shows that it possesses peaks at 2.46 and 2.39 eV; these are phonon sidebands of the electronic transition. This type of weak emission is observed frequently in type-IIa diamond²³ and is termed *H3* luminescence. The *H3* center is one of the most well-studied optical features in diamond, and its presence has been attri-

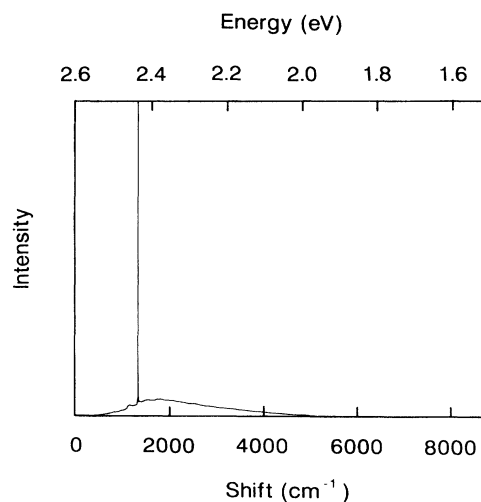


FIG. 2. The Raman/luminescence spectrum of natural unirradiated type-IIa single-crystal diamond. The laser wavelength is 488 nm.

buted to two nitrogen atoms (the *A* aggregate mentioned above) bound to a vacancy.²⁴

The thermal conductivity was measured from 5–300 K along the long direction using a standard steady-state technique.² The absolute uncertainty of the technique is limited by the uncertainty to which the distance between thermocouple sensing probes along the sample length can be measured. We estimate this at 5%.

Neutron irradiation ($E > 0.1$ MeV) was performed at the Phoenix Memorial Laboratory at the University of Michigan for doses up to 1.2×10^{17} neutrons cm^{-2} and at the Research Reactor at the University of Missouri–Columbia for higher doses. The sample was inserted into a quartz tube and exposed to neutron fluences of 3×10^{16} , 1.2×10^{17} , 6.0×10^{17} , and 4.5×10^{18} neutrons cm^{-2} . Because the sample is nearly pure carbon it could be handled almost immediately after removal from the reactor.

III. RESULTS

A. Optical spectra

Figure 3 exhibits the infrared absorbance for both the unirradiated and irradiated diamond. As discussed above, pure diamond shows absorption only in the two- and three-phonon portions of the spectrum because single-phonon absorption is disallowed by symmetry. After the first irradiation a slight absorption edge is barely visible below 1330 cm^{-1} which increases significantly after subsequent irradiation to higher levels. Absorption in this part of the spectrum is due to the presence of defects which disrupt the translational symmetry of the host lattice.²¹ The continuum of absorption in irradiated diamond was first observed by Smith and Hardy⁹ and was attributed to the formation of small regions of disordered carbon material. Several of the peaks in the one-phonon region occur not only in irradiated diamond but also in diamond containing large amounts of impurity nitrogen, indicating that these absorptions are not due to a particular defect or impurity but arise due to maxima in the density of lattice modes. By comparing the magnitude of the 1197-cm^{-1} (0.148-eV) LO-phonon peak in the irradiated material to that present in diamond containing only *A* aggregates (type-IaA diamond),²⁵ one can deduce a lower limit for the total number of carbon atoms ejected from their lattice sites by an impinging neutron;⁹ this value is given in Table I. If these ejected carbon atoms form into

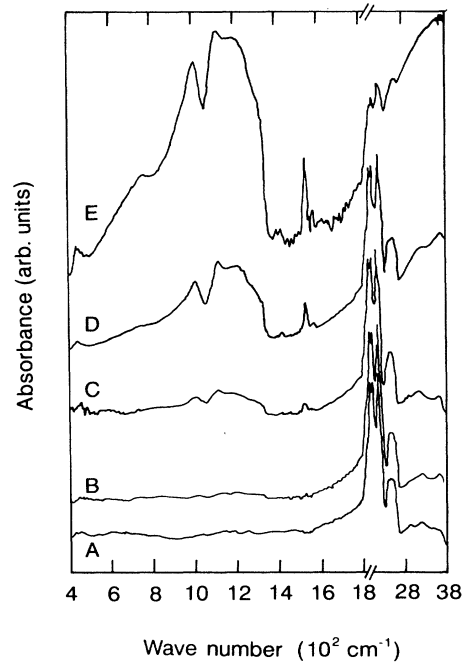


FIG. 3. The infrared absorption of natural unirradiated diamond (curve *A*) and after irradiation to fluences of 3×10^{16} neutrons cm^{-2} (curve *B*), 1.2×10^{17} neutrons cm^{-2} (curve *C*), 6.0×10^{17} neutrons cm^{-2} (curve *D*), and 4.5×10^{18} neutrons cm^{-2} . Note that the abscissa scale emphasizes the single-phonon ($< 1332 \text{ cm}^{-1}$) region of the spectra.

spherically shaped disordered regions, these would have a diameter a_{IR} and density ρ_{IR} given in Table I. An additional feature in the IR spectrum of the irradiated samples is a peak at 1530 cm^{-1} which Woods²⁶ has shown occurs only in irradiated material; this peak is attributed to a localized mode of a primary radiation damage product, presumably a vacancy or carbon interstitial.

Figure 4 exhibits the Raman/photoluminescence spectra of our irradiated diamond. After the first irradiation, we see an increase in the intensity of the *H3* luminescence and the appearance of a new sharp feature at 2.531 eV . This latter feature is irradiation induced and its origin is unidentified at this time; it may arise from the trapping of one or more vacancies at substitutional or *B*-aggregate nitrogen centers. In addition, the Raman line decreases in intensity and broadens to a FWHM of 2.28

TABLE I. Optical parameters of neutron-irradiated diamond single crystal. F is the neutron fluence; N_{IR} is the estimated total number of carbon atoms ejected from their lattice sites; a_{IR} is the estimated spatial extent of disordered region; FWHM is the Raman line full width at half maximum.

F (neutrons cm^{-2})	N_{IR} (atoms cm^{-3})	a_{IR} (Å)	FWHM (cm^{-1})
0	0	0	2.22
3.0×10^{16}	$> 3.0 \times 10^{18}$	> 10.4	2.29
1.2×10^{17}	$> 1.3 \times 10^{19}$	> 10.5	2.46
6.0×10^{17}	$> 4.0 \times 10^{19}$	> 9.1	2.85
4.5×10^{18}	$> 2.0 \times 10^{20}$	> 7.8	7.79

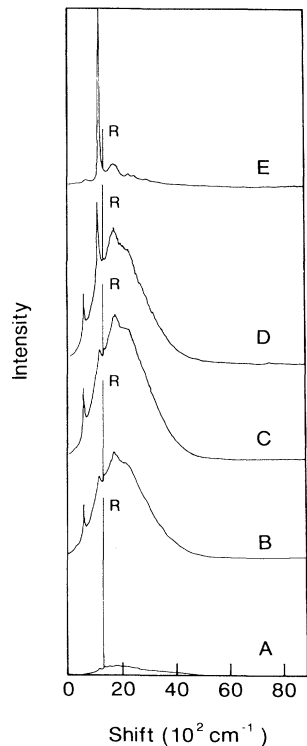


FIG. 4. The Raman/luminescence spectra of irradiated diamond. The sample designation is the same as in Fig. 3. The diamond Raman line (*R*) is indicated.

cm^{-1} but there is no evidence of scattering at higher energies associated with sp^2 -bonded carbon. Also, a small peak develops near 1.673 eV in absolute energy; see Fig. 5. This is a luminescence peak associated with neutral *GR* 1 vacancies which are created when neutrons eject carbon atoms from their lattice sites.²⁷ After the second and third irradiations the *H*3, *GR* 1, and 2.531-eV luminescence centers all grow in intensity and the diamond Raman line continues to weaken and further broaden; as of yet, no feature associated with sp^2 -bonded carbon is observed, however. Upon the final irradiation to a level of 4.5×10^{18} neutrons cm^{-2} some interesting features develop. First, while both the *GR* 1 and 2.531-eV features are observable, the intensities of these peaks are quite small and appear to have saturated. The spectrum is dominated by the *H*3 luminescence features, although the intensity of these peaks appears to be saturating as well. Meanwhile, the Raman intensity is significantly depressed and the linewidth broadens markedly; see Fig. 6 and Table I. In addition we see the appearance of a second rather sharp Raman feature near 1620 cm^{-1} as can be seen in Fig. 7. This small peak is confirmed to be a Raman feature by the invariance of its shifted value of 1620 cm^{-1} with respect to different laser lines.

B. Thermal conductivity

Figure 8 shows the thermal conductivity as a function of temperature for the unirradiated and irradiated specimens. Above 100 K, our data for the thermal conductivi-

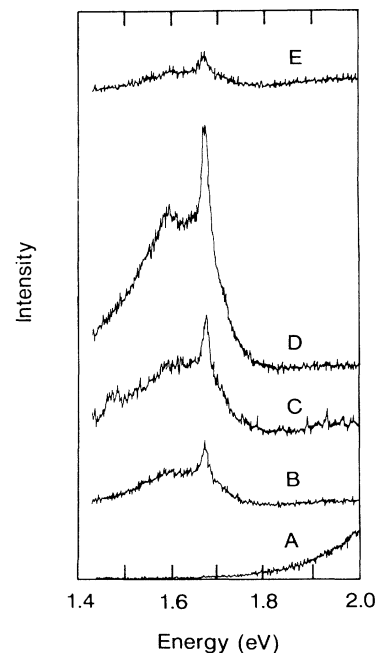


FIG. 5. Luminescence in the range 1.4–2.0 eV in absolute energy showing the *GR* 1 feature at 1.673 eV. The sample designation is the same as in Fig. 3.

ty of natural single-crystal diamond agree with those of Berman and Martinez²⁸ and extrapolate nicely to the recent high-temperature data of Vandersande, Vining, and Zoltan.²⁹ Below 100 K the thermal conductivity of our crystal is less than Berman's; this is the classic size dependence arising from scattering of the heat-carrying phonons from the crystal boundaries, and since our crystal has dimensions smaller than that of Berman the thermal conductivity is smaller in this temperature range. Upon

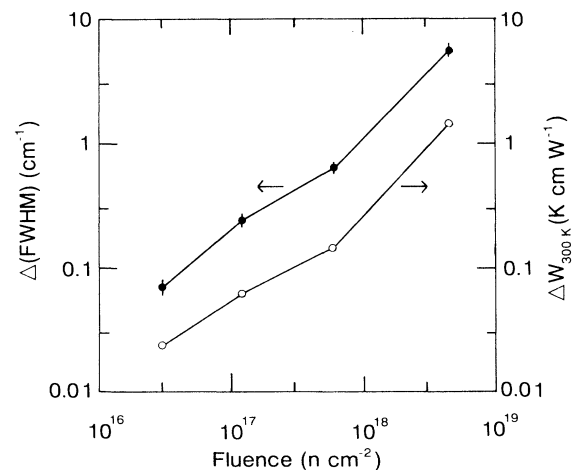


FIG. 6. The change in the Raman diamond linewidth at half maximum ΔFWHM (\bullet) and the change in the room-temperature thermal resistivity ΔW (\circ) as a function of cumulative neutron fluence.

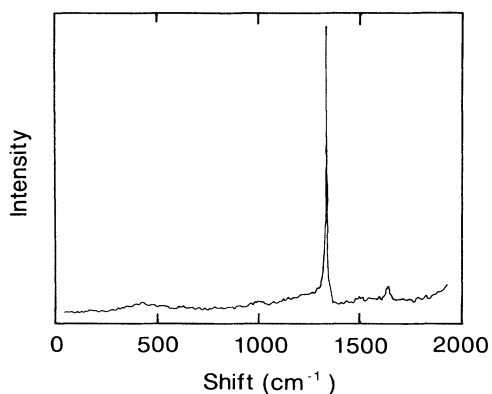


FIG. 7. The Raman spectrum of single-crystal diamond irradiated to a fluence of $4.5 \times 10^{18} \text{ n cm}^{-2}$. Note the appearance of a "glassy carbon" feature at 1620 cm^{-1} .

irradiation to a level of $3 \times 10^{16} \text{ neutrons cm}^{-2}$, the thermal conductivity is dramatically depressed throughout the entire temperature range and the maximum is displaced upward to 250 K; below 30 K, the temperature dependence of κ weakens significantly as the curve begins to approach that of the unirradiated material. After subsequent irradiations the thermal conductivity is depressed even further, and the bending at low temperature is even more pronounced. Figure 6 shows the behavior of the additional thermal resistivity of the irradiated specimens above that of the pristine sample versus dose. The strong increase in ΔW for the fourth irradiation mirrors the increase in the FWHM of the Raman line for this dose. In fact, a plot of the change in the

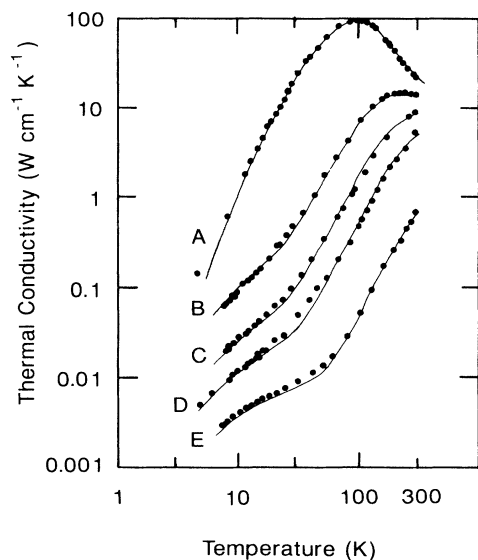


FIG. 8. The thermal conductivity of natural and irradiated single-crystal diamond. The curve designation is the same as in Fig. 3. The solid lines are fits to the data as described in the text.

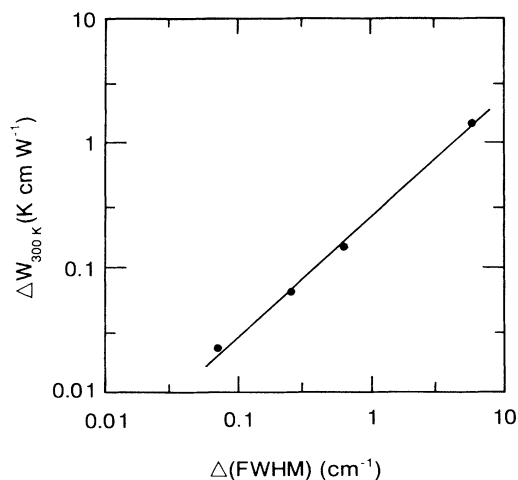


FIG. 9. The change in the room-temperature thermal resistivity ΔW as a function of the change in the Raman diamond linewidth at half maximum ΔFWHM .

resistivity at 300 K versus the change in Raman linewidth (Fig. 9) shows a linear behavior, with $\Delta W \text{ (cm K W}^{-1}) \approx 0.25 [\Delta \text{FWHM (cm}^{-1})]$.

IV. DISCUSSION

A. Production of radiation-damage and optical spectra

From previous studies of the infrared absorption⁹ and x-ray diffraction^{10,11} of neutron-irradiated diamond together with the optical spectra presented here, one can form the following picture of the irradiation process: For low fluences, neutrons eject carbon atoms from their lattice sites, thereby creating vacancies. The number of displaced carbon atoms, or primary knock-ons, produced per unit volume in the bombardment is³⁰

$$N_p = F n_0 \sigma, \quad (1)$$

where F is the neutron fluence, n_0 the number of carbon atoms per unit volume, and σ the cross section for collisions. For diamond, $n_0 = 1.76 \times 10^{23} \text{ cm}^{-3}$ and $\sigma \approx 4 \text{ b}$ for neutron energies between 0.1 and 1 MeV.³¹ Thus $N_p \approx 0.7 F$, i.e., nearly one primary knock-on is produced for each incident neutron. The average energy transferred to a carbon atom by a neutron of energy E is³²

$$\Delta E = 2ME / (M + 1)^2, \quad (2)$$

where M is the carbon atomic mass in mass units. For a 1-MeV neutron this yields $\Delta E = 140 \text{ keV}$. Since it takes approximately 37 eV to remove a carbon atom from the diamond lattice for a neutron projected along the [100] axis,³³ clearly one incident neutron is capable of ejecting several carbon atoms. Using such considerations, Dienes and Kleinman³⁴ have shown that the energetic recoil atoms rupture covalent single bonds which subsequently reform into a disordered region of double and single bonds. They estimate that each incident neutron creates

a disordered region approximately 45 Å in diameter consisting of some 10^4 carbon atoms. The formation of disordered regions by ejected interstitial carbon atoms is consistent with the high mobility of the carbon interstitial at and even below room temperature.³⁵ These disordered regions of sp^2 -bonded carbon give rise to the one-phonon infrared absorption observed in Fig. 3. The size of the disordered region and the number of carbon atoms involved is somewhat larger in Dienes and Kleinman's model than that estimated from the infrared absorption (Table I). This difference is most likely due to two factors: (a) the estimate from the intensity of infrared absorption of the total number of radiation-induced defects gives only a lower limit since it assumes that the dipole coupling of these defects is as strong as that due to *A*-aggregate nitrogen, which is probably unlikely; and (b) the radiation-damage model predictions depend strongly on the actual incident neutron energy; energies smaller than those used by Dienes and Kleinman will produce disordered regions consisting of fewer atoms and of smaller spatial extent. For example, for an incident neutron energy of 1 MeV, simple radiation-damage models^{30,32} predict that a total of $\sim 10^3$ carbon atoms will be removed from their lattice sites for each incident neutron. If these form into spherically shaped regions, the spatial extent of these would be about 20 Å.

The increase in intensity of the luminescence features at 1.673 and 2.463 eV at low doses gives clear evidence of the creation of vacancies in the irradiated diamond, and also suggests that a portion of the *A*-aggregate nitrogen existed as nitrogen pairs and not as *H3* centers (*N-V-N* complexes) prior to irradiation. Thus at least some fraction of the vacancies created by irradiation migrate to the *A* aggregates to produce the *H3* luminescence feature, a process recently proposed by Lawson *et al.*³⁶ On the other hand, at the highest dose level it appears that the *GR1* and *H3* features saturate, implying that the vacancies are involved in more complicated arrangements such as clusters or interstitial/vacancy aggregates. Prins³⁷ has shown that the most likely radiation-damage products for *ion-bombarded* diamond are vacancy clusters and these may begin to occur in our sample irradiated to 4.5×10^{18} neutrons cm^{-2} .

The strong decrease in intensity and broadening of the diamond phonon line are indicative of the growing disorder in the lattice. This disorder also manifests itself in the appearance of the second weak Raman line at 1620 cm^{-1} . This line is characteristic of "glassy" carbons and microcrystalline graphite of very small ($< 25\text{-}\text{Å}$) grain size³⁸ and provides strong evidence for the existence of small regions of essentially amorphous material. Thus it would appear that at least some of the ejected carbon atoms have reformed themselves into highly disordered regions of sp^2 -bonded carbon, with the possible incorporation of vacancies as well.

B. Thermal conductivity

One might expect that disordered regions will scatter phonons independently of frequency at high temperature (when the phonon wavelength λ is small compared to the

size of the region), but that this scattering will fade away at low temperature when the phonon wavelength is long compared to the defect size. In addition, vacancies created by the removal of carbon atoms from lattice sites, as observed by the onset of luminescence at 1.673 eV, will provide additional point defect scattering of phonons. Klemens³⁹ has considered theoretically the influence of neutron irradiation on the thermal conductivity of insulators, including the effects of both point and extended defects. The basic conclusions of his study are that point defects will degrade the thermal conductivity at high temperatures (above the maximum), while the extended defects depress the thermal conductivity to temperatures well below the maximum in thermal conductivity of the unirradiated specimen.

One can quantify the influence of defects on the thermal conductivity by analyzing the curves using the Debye model. Accordingly, the phonon thermal conductivity of a crystal is given by

$$\kappa = \frac{\hbar^2}{2\pi^2 k_B v T^2} \int_0^{\omega_D} \frac{\omega^4 \tau(\omega) \exp(\hbar\omega/k_B T) d\omega}{[\exp(\hbar\omega/k_B T) - 1]^2} . \quad (3)$$

Here $v = 1.32 \times 10^4 \text{ m s}^{-1}$ is the phonon velocity,⁴⁰ ω the phonon frequency, $\omega_D = k_B \theta / \hbar$ ($\theta = 2050 \text{ K}$ is the Debye temperature⁴¹), and τ the total phonon-scattering time. In the presence of many scattering processes, one must add the corresponding scattering rates and then take the inverse of this sum to obtain the total scattering time. For the situation considered here, the following scattering rates must be included.⁴²

(1). Phonon-phonon umklapp scattering (τ_u^{-1}). The form suggested by Glassbrenner and Slack⁴³ for silicon and germanium, which are isostructural to diamond, is preferred here:

$$\tau_u^{-1}(\omega) = B \omega^2 T \exp(-\theta/bT) . \quad (4)$$

This form is different from that used by Berman and Martinez,²⁸ but as pointed out recently by Graebner and Herb⁵ and Onn *et al.*,⁴⁴ it provides a better fit to the recent high-temperature data²⁹ than the *U*-process rate used by Berman, and is somewhat better justified on theoretical grounds.

(2). Phonon-boundary scattering (τ_b^{-1}). The scattering of phonons from the boundaries of the crystal is the dominant scattering mechanism at low temperature when the phonon wavelength approaches the specimen size.⁴⁵ For diffuse scattering at the boundary this rate is frequency independent:

$$\tau_b^{-1}(\omega) = v/1.12d , \quad (5)$$

where $d = 0.77 \text{ mm}$ is the effective sample diameter corrected for the finite sample length.⁴⁶ Since this rate is frequency (and thus temperature) independent, one expects that the low-temperature thermal conductivity will display the same temperature dependence as the specific heat, i.e., $\kappa \sim T^3$.

(3). Phonon-point defect scattering (τ_p^{-1}). Point defects scatter phonons with a Rayleigh-type frequency dependence:⁴⁷

TABLE II. Parameters used to fit the thermal conductivity of pristine and neutron-irradiated diamond. F is the neutron fluence; B is the U -process scattering-rate coefficient; b is the U -process exponent [see Eq. (4)]; P is the point defect scattering-rate coefficient [see Eq. (6)]; a is the extended defect diameter; ρ_T is the extended defect concentration.

F (neutrons cm^{-2})	B (s K^{-1})	b	P (s^3)	a (\AA)	ρ_T (cm^{-3})
0	2.9×10^{-20}	3.2	1.0×10^{-46}	0	0
3.0×10^{16}	2.9×10^{-20}	3.2	1.7×10^{-46}	16	4.5×10^{16}
1.2×10^{17}	2.9×10^{-20}	3.2	2.3×10^{-46}	16	1.9×10^{17}
6.0×10^{17}	2.9×10^{-20}	3.2	2.7×10^{-46}	17	1.0×10^{18}
4.5×10^{18}	2.9×10^{-20}	3.2	3.4×10^{-46}	11	5.6×10^{19}

$$\tau_p^{-1}(\omega) = P\omega^4. \quad (6)$$

In natural diamond, the main point defects are carbon isotopes and nitrogen impurities. In irradiated material the point defect rate will be increased due to the production of vacancies.

(4). Phonon-extended defect scattering (τ_e^{-1}). As discussed above, extended defects scatter phonons geometrically (i.e., like boundaries) for small phonon wavelengths and Rayleigh-like (i.e., like point defects) for large phonon wavelengths. In particular, one has⁴⁸

$$\begin{aligned} \tau_e^{-1}(\omega) &= \rho_T v \pi a^2 / 4 \quad \text{for } qa > 1 \\ &= C\omega^4 \quad \text{for } qa < 1. \end{aligned} \quad (7)$$

Here a is the radius of the defect (assumed spherical), ρ_T is the extended defect concentration (as determined from the thermal conductivity), q is the phonon wave vector, and $C = \rho_T \pi a^6 / 4v^3$.

The procedure we use is to fit the data of the natural unirradiated diamond with scattering rates (4), (5), and (6), and then include additional point defect scattering as well as extended defect scattering to fit the data of the irradiated samples, leaving the rates for boundary and umklapp scattering unchanged from those of the unirradiated crystal. The parameters used to fit the data of the pristine diamond are given in Table II. The value for b is similar to that for silicon and germanium, for which $b \approx 3.0$.⁴³ According to Slack and Galginaitis,⁴⁹ the coefficient of the umklapp term B is given by

$$B = \hbar\gamma^2 / Mv^2\theta. \quad (8)$$

This yields the value $\gamma = 1.18$ for diamond, which compares favorably with the value of $\gamma \approx 0.9$ determined from high-temperature thermal-expansion measurements.⁵⁰ For carbon-13 isotopes at the naturally occurring level of 1%, one expects $P = 1.34 \times 10^{-47} \text{ s}^3$. The value found here is almost the same as that found by Berman and Martinez ($P = 1.17 \times 10^{-46} \text{ s}^3$), and as discussed by those authors²⁸ the extra point defect scattering is consistent with that due to small aggregates of nitrogen. Thus we have obtained an excellent fit to the thermal conductivity of unirradiated diamond (see the solid line in Fig. 8) from 7–1000 K using just three scattering rates with very reasonable values for the adjustable parameters. The task now is to fit the data of the irradiated specimen including point and extended defects and guid-

ed by the observations in the optical spectra.

Figure 8 shows the fit to the thermal conductivity of the irradiated diamond achieved by including the effect of extended defects. We would like to stress that the fits to the irradiated samples use the same boundary and umklapp scattering rates as for the unirradiated diamond. The parameters used in the fits are shown in Table II. The spatial extent a of the disordered region, which is determined by the location of the knee in the thermal-conductivity curve, also is close to that estimated from the infrared absorption (Table I) and is nearly the same as the value predicted by radiation-damage models.^{30,32} The concentration of disordered regions as determined from the thermal conductivity increases strongly after the final irradiation (Fig. 10) and is similar to the behavior seen in Fig. 6 for the increase in thermal resistivity at 300 K and the change in the Raman linewidth. Taken together these results suggest that the induced damage becomes more severe than for doses up to $6 \times 10^{17} \text{ neutrons cm}^{-2}$, and is probably related to the saturation of the “simple”

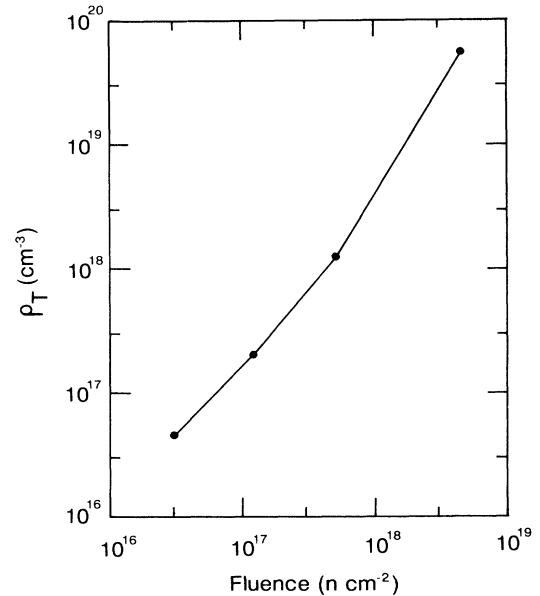


FIG. 10. The concentration of disordered regions ρ_T as determined from the thermal conductivity as a function of neutron fluence.

vacancy-related defects *GR* 1 and *H*3 and an increase in the concentration of more extended defective regions involving both interstitials and vacancies. While the point defect scattering-rate coefficient determined from the fit to the conductivity also appears to increase with the dose, probably due to an increase in vacancy concentration, we attempt no correlation between this and the irradiation dose because the thermal-conductivity curves for the irradiated specimens are very insensitive to this term, most of the additional scattering being due to the extended defects.

We can conclude from the optical and thermal-conductivity results that, at low levels of irradiation, some of the vacancies produced are isolated *GR* 1 centers, while others are trapped at *A*-aggregate nitrogen. Meanwhile, the displaced carbon atoms form into disordered regions (on the order of one such region being produced per incident neutron) of spatial extent on the order of 15 Å. For irradiation up to 4.5×10^{18} neutrons cm^{-2} , the *GR* 1 and *H*3 features saturate, indicating that all newly created vacancies become incorporated into more complicated defect structures. It is proposed that the vacancies and ejected carbon atoms form disordered regions of sp^2 -bonded carbon, and the concentration of these regions increases strongly once the *H*3 and *GR* 1 sinks for vacancies are saturated.

C. Comparison with diamond films

A major impetus for carrying out the present study was to shed light on the role played by defects in the thermal conductivity of diamond films. Morelli, Hartnett, and Robinson⁴ showed that the thermal conductivity of films grown by a hot-filament (HF) process is lower than that of films grown by a microwave (*M*) process, even though the two types of films had nearly the same crystallite size; see Fig. 11. The diminution of κ in the HF films was due mainly to a depression in the thermal conductivity in the range 15–60 K. Such dips in the thermal conductivity have been observed in nearly all HF samples studied,^{2,4,51} and also occasionally in *M* samples as well.⁵ It is clear from the above results that small regions of disordered carbon material in the diamond lattice are capable of producing precisely this effect. In fact, a comparison of the infrared spectra of the films measured in Ref. 4 shows that the HF samples exhibit single-phonon absorption due to regions of sp^2 -bonded carbon⁵² which is almost identical to that observed in irradiated single crystals. Thus it seems likely that these very small regions of disorder are responsible to a large extent for the observed thermal conductivity of the HF films. While resonant scattering from vacancies could provide an alternative explanation of the thermal conductivity of both irradiated diamond and HF diamond films, two observations lead us to reject this hypothesis. First, the location in temperature of the dip in the thermal conductivity differs slightly from film to film and from film to irradiated single crystal. This is consistent with the size of the disordered region being slightly different from sample to sample. If the active mechanism were a resonant interaction, one would expect the dip always to occur at the

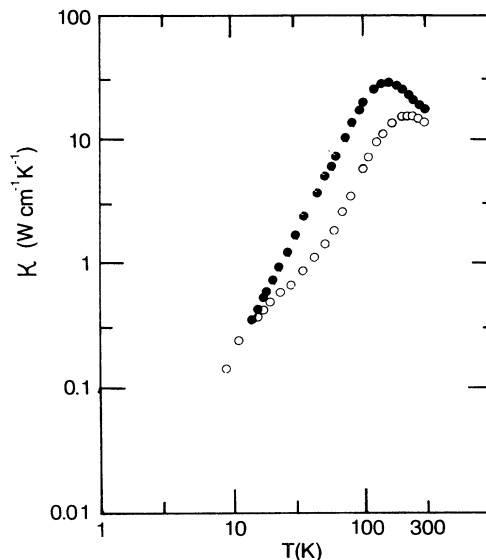


FIG. 11. The thermal conductivity of hot-filament (●) and microwave-plasma-assisted (○) vapor-deposited diamond films from Ref. 4.

same temperature corresponding to the dominant phonon energy equal to the characteristic energy of the resonance. Second, recent measurements on *electron-irradiated* diamond, for which principally only neutral vacancies and interstitials are created, showed no such dip in the thermal conductivity in this temperature range.⁵³

It is quite interesting to note that the existence of a very small amount of disordered carbon in either a film or an irradiated diamond will dramatically depress the thermal conductivity even though its presence is not revealed by a peak in the sp^2 portion of the Raman spectrum. It seems, rather, that absorption in the single-phonon portion of the infrared spectrum is a more sensitive tool for detecting the presence of disordered carbon than Raman scattering. Thus it does not appear possible, at least for low sp^2 carbon concentrations, to make a correlation between thermal conductivity of a diamond film and the ratio of the sp^2 and sp^3 carbon Raman peak intensities, as has been suggested.¹ Perhaps the most sensitive tool of any for the detection of disordered carbon in diamond is the thermal conductivity itself; disordered carbon at a concentration barely high enough to be detected by infrared absorption and invisible in the Raman spectrum is capable of decreasing the thermal conductivity of a single crystal by 40% at room temperature and by a factor of 50 at 30 K. This is largely a matter of coincidence: from 30 to 300 K the thermal conductivity of diamond is most sensitive to the presence of defects, because phonon-phonon scattering is not yet the dominant interaction.

Because diamond amorphizes at high neutron doses, it would be of interest to study the nature of heat transport in this regime as well. Such experiments are currently underway.

ACKNOWLEDGMENTS

The authors thank Dr. Joseph Heremans, Professor Jean-Paul Issi, and Professor Paul Klemens for fruitful discussions. We also thank David McEwen for the infrared spectra and Philip Simpson for performing the irradiations at the University of Michigan.

- ¹A. Ono, T. Baba, H. Funamoto, and A. Nishikawa, *Jpn. Appl. Phys.* **25**, L808 (1986).
- ²D. T. Morelli, C. P. Beetz, and T. A. Perry, *J. Appl. Phys.* **64**, 3063 (1988).
- ³J. A. Herb, C. Bailey, and P. A. Dennig, in *Proceedings of the Electrochemical Society*, edited by J. P. Dismukes (The Electrochemical Society, Pennington, NJ, 1989), Vol. 89-12, p. 366.
- ⁴D. T. Morelli, T. M. Hartnett, and C. J. Robinson, *Appl. Phys. Lett.* **59**, 2112 (1991).
- ⁵J. E. Graebner and J. A. Herb, *Diam. Films Tech.* **1**, 155 (1992).
- ⁶V. I. Nepsha, N. F. Reshetnikov, Yu. A. Klyuev, G. B. Bokii, and Yu. A. Pavlov, *Dok. Akad. Nauk. SSSR [Sov. Phys. Dokl.]* **30**, 1275 (1985).
- ⁷J. E. Graebner, S. Jin, G. W. Kammlott, J. A. Herb, and C. F. Gardinier, *Appl. Phys. Lett.* **60**, 1576 (1992).
- ⁸C. D. Clark, R. W. Ditchburn, and H. B. Dyer, *Proc. R. Soc. London, Ser. A* **237**, 75 (1956).
- ⁹S. D. Smith and J. R. Hardy, *Philos. Mag.* **5**, 1311 (1960).
- ¹⁰E. R. Vance, *J. Phys. C* **4**, 257 (1971).
- ¹¹P. W. Levy and O. F. Kammerer, *Phys. Rev.* **100**, 1787 (1956).
- ¹²R. Berman, E. L. Foster, and H. M. Rosenberg, in *Defects in Crystalline Solids—A Report on the 1954 Bristol Conference*, edited by A. C. Stickland (The Physical Society, London, 1954), p. 321.
- ¹³W. H. Reichelt, W. A. Ranken, C. V. Weaver, A. W. Blackstock, A. J. Patrick, and M. C. Chaney, in *Proceedings of the Thermionics Conversion Specialists Conference, Miami, Florida, 1970*, edited by G. Wade (Institute of Electrical and Electronics Engineers, New York, 1971), p. 39.
- ¹⁴G. Pompe, N. Abdel-Rehim, and M. Mertig, *J. Low-Temp. Phys.* **74**, 475 (1989).
- ¹⁵R. Berman, *Proc. R. Soc. London, Ser. A* **208**, 90 (1951); *Adv. Phys.* **2**, 864 (1953).
- ¹⁶J. W. Gardner and A. C. Anderson, *Phys. Rev. B* **23**, 474 (1981).
- ¹⁷A. M. deGoer, N. Devismes, and B. Salce, in *Phonon Scattering in Condensed Matter V*, edited by A. C. Anderson and J. P. Wolfe (Springer, Berlin, 1986), p. 70.
- ¹⁸G. Davies, *Chem. Phys. Carbon* **13**, 1 (1976).
- ¹⁹The only published data on the thermal conductivity of neutron-irradiated diamond are that of Berman *et al.* on a type-Ia crystal (see Ref. 10). They report, without further comment or analysis, that after an irradiation at a level of 1×10^{18} neutrons cm^{-2} , "in the liquid hydrogen region (the thermal conductivity) has decreased by a factor of $\frac{1}{180}$, and at 90 K it is still only one-fiftieth of that of the unirradiated specimen."
- ²⁰M. Lax and E. Burstein, *Phys. Rev.* **97**, 39 (1955).
- ²¹C. A. Klein, T. M. Hartnett, R. P. Miller, and C. J. Robinson, in *Proceedings of the 2nd International Conference on Diamond Materials*, edited by A. J. Purdes, J. C. Angus, R. F. Davis, B. M. Meyerson, K. E. Spear, and M. Yoder (Electrochemical Society, Pennington, NJ, 1991), p. 435.
- ²²S. A. Solin and A. K. Ramdas, *Phys. Rev. B* **1**, 1687 (1970).
- ²³C. D. Clark, R. W. Ditchburn, and H. B. Dyer, *Proc. R. Soc. London, Ser. A* **234**, 363 (1956).
- ²⁴G. Davies, in *Diamond Research 1976* (Industrial Diamond Information Bureau, London, 1976), p. 15.
- ²⁵G. S. Woods, G. C. Purser, A. S. S. Mtimkulu, and A. T. Collins, *J. Phys. Chem. Solids* **51**, 1191 (1990).
- ²⁶G. S. Woods, *Philos. Mag. B* **50**, 673 (1984).
- ²⁷J. E. Lowther and A. M. Stoneham, *J. Phys. C* **11**, 2165 (1978).
- ²⁸R. Berman and M. Martinez, in *Diamond Research 1976* (Ref. 24), p. 7.
- ²⁹J. W. Vandersande, C. B. Vining, and A. Zoltan (unpublished).
- ³⁰G. J. Dienes and G. H. Vineyard, *Radiation Effects in Solids* (Interscience, New York, 1957), p. 28.
- ³¹D. I. Garber and R. R. Kinsey, *Neutron Cross Sections* (Brookhaven National Laboratory Associated Universities, Inc., Upton, New York, 1976), Vol. II, p. 28.
- ³²F. Seitz, *Discussions Faraday Soc.* **5**, 271 (1949).
- ³³J. Koike, D. M. Parkin, and T. E. Mitchell, *Appl. Phys. Lett.* **60**, 1450 (1992).
- ³⁴G. J. Dienes and D. A. Kleinman, *Phys. Rev.* **91**, 238 (1953).
- ³⁵J. Koike, T. E. Mitchell, and D. M. Parkin, *Appl. Phys. Lett.* **59**, 2515 (1991).
- ³⁶S. Lawson, G. Davies, A. T. Collins, and A. Mainwood, *J. Phys. Condens. Matter* **4**, L125 (1992).
- ³⁷J. F. Prins, *Phys. Rev. B* **38**, 5576 (1988).
- ³⁸R. J. Nemanich and S. A. Solin, *Phys. Rev. B* **20**, 392 (1979).
- ³⁹P. G. Klemens, *Nucl. Instrum. Methods B* **1**, 204 (1984).
- ⁴⁰J. W. Vandersande, *Phys. Rev. B* **13**, 4560 (1976).
- ⁴¹G. A. Slack, in *Solid State Physics*, edited by H. Ehrenreich, F. Seitz, and D. Turnbull (Academic, New York, 1979), Vol. 34, p. 1.
- ⁴²We neglect the inclusion of normal phonon-phonon processes as described by the Callaway model. The presence of nitrogen-related defects in the unirradiated specimen and the large concentration of defects in the irradiated samples ensures that resistive processes are always present and render the effect of normal processes negligible.
- ⁴³C. J. Glassbrenner and G. A. Slack, *Phys. Rev.* **134**, A1058 (1964).
- ⁴⁴D. G. Onn, A. Witek, Y. Z. Qiu, T. R. Anthony, and W. F. Banholzer, *Phys. Rev. Lett.* **68**, 2806 (1992).
- ⁴⁵H. B. G. Casimir, *Physica* **5**, 495 (1938).
- ⁴⁶R. Berman, F. E. Simon, and J. M. Ziman, *Proc. R. Soc. London, Ser. A* **220**, 171 (1953).
- ⁴⁷P. G. Klemens, *Proc. Phys. Soc. London, Sect. A* **68**, 1113 (1955).
- ⁴⁸J. W. Vandersande, *Phys. Rev. B* **15**, 2355 (1977).
- ⁴⁹G. A. Slack and S. Galgaitis, *Phys. Rev.* **133**, A253 (1964).
- ⁵⁰D. Gerlich, *J. Chem. Phys. Solids* **35**, 1026 (1974).
- ⁵¹T. R. Anthony, J. L. Fleischer, J. R. Olson, and D. G. Cahill, *J. Appl. Phys.* **69**, 8122 (1991).
- ⁵²C. J. Robinson (private communication).
- ⁵³D. T. Morelli (unpublished).